Motor Coordination Learning for Rhythmic Movements

Melanie Jouaiti, Patrick Henaff

Motor Coordination Learning for Rhythmic Movements

Melanie Jouaiti[1] and Patrick Henaff[2]

***Abstract*— The perspective of ubiquitous robots raises the issue of social acceptance. It is our belief that a successful robot integration relies on adequate social responses. Human social interactions heavily rely on synchrony which leads humans to connect emotionally. It is henceforth, our opinion, that motor coordination mechanisms should be fully integrated to robot controllers, allowing coordination, and thus social synchrony, when required. The aim of the work presented in this paper is to learn motor coordination with a human partner performing rhythmic movements. For that purpose, plastic Central Pattern Generators (CPG) are implemented in the joints of the Pepper robot. Hence, in this paper, we present an adaptive versatile model which can be used for any rhythmic movement and combination of joints. This is demonstrated with various arm movements.**

I. Introduction

In the last few years, social robotics has been widely developed with the problematic of how to make robots more acceptable. The question has been considered from pretty much every angle, by trying to make the robots physically attractive to humans, by working on robot gaze, robot speech, robot grasping or robot walk. Another aspect, which should not be neglected is the social adequacy and especially the synchrony phenomena which tend to emerge consciously, or unconsciously when humans interact with each other [1], while walking [2], rocking chairs [3] or handshaking [4]. As it just so happens, rhythmic gestures inherently induce dynamic coupling phenomena playing a fundamental role in physical and social interpersonal interactions [5], [6].

While the term *coordination* refers to two events occurring with a constant phase difference (which can differ from zero), the term *synchronization* is more restrictive and imposes a phase difference of 0 or π. So synchronization between a robot and a human performing rhythmic movements would necessarily lead to motor coordination.

In our opinion, should a robot have the ability to respond in a socially acceptable way in rhythmic interactions, i.e. to adapt to the human, robot controllers able to produce rhythmic movements and trigger the emergence of motor coordination in the interaction are required. One chosen way to achieve this consists in designing intrinsically rhythmic bio-inspired robot controllers, such as Central Pattern Generators (CPGs) which also incorporate synchronization learning abilities similarly to the plasticity mechanisms involved in the human motor nervous system for rhythmic movements production and coordination.

The aim of this work is to learn motor coordination with a human partner performing rhythmic arm movements with changing frequency, amplitude and motion. Consequently, plastic CPGs, i.e. CPGs which incorporate plasticity mechanisms, are implemented in the joints of the Pepper robot. Results show that the robot is indeed able to achieve motor coordination with the human performing various arm motions.

In the second part of this paper, related works are presented. In the third part, the CPG model, its architecture and the equations used in this work are introduced. Then, in the fourth part, the experimental setup as well as the experimental results are presented. Finally, we discuss our results.

II. Related Works

In [7], subjects were asked to wave their hand to the beat of a metronome while the experimenter uttered disruptive words and either waved her hand in phase or anti-phase or not at all. It was observed that subjects remembered more words and attributed a greater likability to the experimenter when she was waving in phase. In [8], a robotic arm was able to synchronize with an external signal and perform coordinated drum beating with a changing frequency. They employed the Dynamic Movement Primitives Framework presented in [9].

Closer to this work, [10] introduced a model designed to reproduce rhythmic arm movements with the NAO robot. A reservoir of oscillators provides one with a close frequency and while the oscillator can be slightly entrained during the interaction, the oscillators do not retain the frequency, going back to their original properties right afterwards.

A CPG is a biological structure found in the spinal cord of vertebrates. It can generate a rhythmic signal which can be modulated by sensory feedbacks, without receiving any rhythmic input. The role of CPGs in locomotion has been proven and well studied and its implication in rhythmic upper limb movements is also strongly suspected [11], [12]. CPGs are based on a pair of two mutually inhibitory oscillating neurons, called half-center [13], controlling the extensor and flexor muscles. Non-linear CPGs, also called relaxation oscillators, can synchronize with an oscillatory input or with a coupled CPG, thus ensuring coordination.

Several oscillator models can produce movement coordination [14], [15]. We chose the Rowat-Selverston (RS) oscillating neuron model [16] which can exhibit the four characteristic behaviors of a biological neuron, i.e. endogenous bursting, plateau potential, post-inhibitory rebound and

*This work was supported by CPER 2015-2020, plateform IT2MP-SCIARAT, region Nancy Grand-Est, France

[1]Melanie Jouaiti is with Université de Lorraine, CNRS, LORIA, F-54000 Nancy, France melanie.jouaiti@loria.fr

[2]Patrick Hénaff is with Université de Lorraine, CNRS, LORIA, F-54000 Nancy, France patrick.henaff@loria.fr

quiescence [17], [18].

Moreover, McCrea and Rybak [19] proposed a bio-inspired model of half-center CPG for mammal locomotion. The CPG is divided into the extensor and flexor parts and has four interneuron layers: Rhythm Generator, Pattern Formation, Sensory Neurons and Motoneurons. It can also takes sensory feedback into account. While this model is widely used for locomotion [20], [21], [22], very few works apply it to arm movements: to our knowledge, only [23] used it to study the reaching movement.

III. Materials and Methods

A. CPG Architecture

The general architecture for the CPG is represented Fig. 1. In the experiments presented in this article, a SoftBank Robotics Pepper robot is used. The output of the CPG is thus considered as an angular position offset and the position control mode to command the joints of Pepper is employed. For a better understanding of this subsection, please refer to [24] where the CPG model is extensively detailed.

1) Mathematical Models of the neurons: For the rhythm generator neurons, Rowat-Selverston cells are used. Forcing the oscillator and adding mutual inhibition between the rhythmic cells, the RS neuron model can be written as follows:

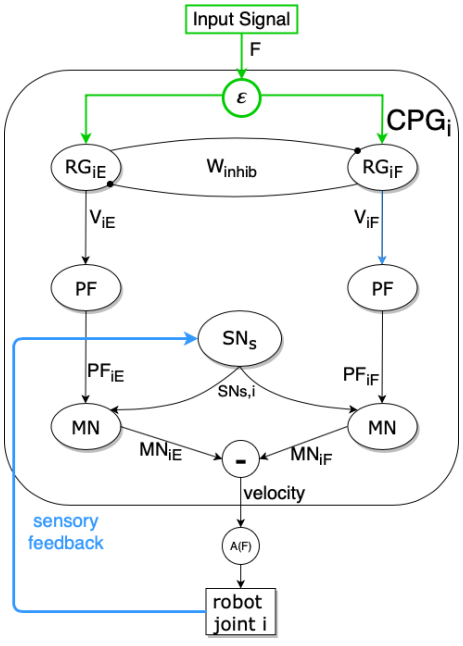

Fig. 1. General CPG architecture. The CPG output values are used as angular position commands. With $A(F)$ the amplitude of F

$$\dot{V}_{i_{\{E,F\}}} = y_{i_{\{E,F\}}} - W\frac{y_{i_{\{E,F\}}}}{1+e^{-4y_{i_{\{F,E\}}}}} + \epsilon_{i_{\{E,F\}}}F_i \tag{1}$$

$$\dot{y}_{i_{\{E,F\}}} = \left(\sigma_f - \frac{\tau_m}{\tau_s} - 1 - \sigma_f \tanh^2\left(\frac{\sigma_f}{A_{f_{i_{\{E,F\}}}}}V_{i_{\{E,F\}}}\right)\right)\cdot \frac{y_{i_{\{E,F\}}}}{\tau_m} - \frac{1+\sigma_{s_{i_{\{E,F\}}}}}{\tau_s\tau_m}V_{i_{\{E,F\}}} + \frac{A_{f_{i_{\{E,F\}}}}}{\tau_s\tau_m}\tanh\left(\frac{\sigma_f V_{i_{\{E,F\}}}}{A_{f_{i_{\{E,F\}}}}}\right) \tag{2}$$

with V the membrane potential and τ_m and τ_s time constants, A_f influences the output amplitude, while σ_f determines whether the neuron is able to oscillate or not. σ_s influences the intrinsic frequency, $i \in \mathbb{N}$, designating the joint id. F_i the CPG input, ϵ a synaptic weight designed to scale the input and the term in W models the mutual inhibition between the extensor and flexor rhythmic cells.

Pattern Formation neuron PF, Sensory neuron SN and Motoneurons MN are defined as follows [24]:

$$PF(V_{i_{\{E,F\}}}) = PF_{i_{\{E,F\}}} = \frac{1}{1+e^{\frac{-V_{i_{\{E,F\}}}}{2}}} \tag{3}$$

$$SN(v_{mes_i}) = SN_i = \frac{1}{1+e^{\alpha_s pos_{i_{mes}}}} \tag{4}$$

$$MN(PF_{i_{\{E,F\}}}, SN_i) = MN_{i_{\{E,F\}}} = \frac{1}{1+e^{\alpha_m\left(PF_{i_{\{E,F\}}} - SN_i\right)}} \tag{5}$$

with $\alpha_s = -0.061342$ and $\alpha_m = 3$. pos_{mes_i} is the angular position measured for the given joint.

While MN_{i_F} and MN_{i_E} would be the command of the flexor and extensor muscles respectively in biological systems, in robotics, it is customary to subtract both signals. So the output would be:

$$output_i(t) = MN_{i_F} - MN_{i_E} \tag{6}$$

B. Plasticity mechanisms

Since the RS model is a generalized Van der Pol oscillator, known properties of the Van der Pol can be applied. Hebbian mechanisms inspired by [25] can be integrated to the bio-inspired CPGs, enabling it to learn an external signal.

The learning rules proposed in [24] can be applied and frequency learning, inspired by [25], is defined as:

$$\dot{\sigma}_{s_{i_{\{E,F\}}}} = 2\epsilon_{i_{\{E,F\}}}F_i\sqrt{\tau_m\tau_s(1+\sigma_{s_{i_{\{E,F\}}}} - \sigma_f)}\cdot \frac{y_{i_{\{E,F\}}}}{\sqrt{V^2_{i_{\{E,F\}}} + y^2_{i_{\{E,F\}}}}} \tag{7}$$

In equation 1, the expression $A_f \tanh(\frac{\sigma_f}{A_f}V)$ influences the amplitude of V and hence of the CPG output. It is thus

interesting to adapt the amplitude of the neuron oscillations in accordance with the applied signal F_i. The learning rule for the amplitude A_f is the following:

$$\dot{A}_{f_{i_{\{E,F\}}}} = -\mu \left(\left(\frac{\nu \sigma_f V_{i_{\{E,F\}}}}{A_{f_{i_{\{E,F\}}}}} \right)^2 - {F_i}^2 \right) \tag{8}$$

Finally, ϵ can be considered as a synaptic weight that normalizes the external signal F_i. The adaptation of ϵ is realized with:

$$\dot{\epsilon}_{i_{\{E,F\}}} = \lambda tanh^2(\xi F_i) \left(1 - (\epsilon_{i_{\{E,F\}}} F_i)^2\right) \tag{9}$$

μ and λ are learning steps. ν and ξ are scaling factors.

C. Modular Architecture

In human vision, starburst cells are important in the computation of direction-selectivity [26]. Those are interneurons which respond to a visual stimulus moving in a specific direction. In this work, we replicate this behavior with the CPGs, making them direction-specific. The shoulder pitch receives the vertical component of the hand position as an input and the shoulder roll receives the horizontal component. In the present experiments, three joints of the left arm, the shoulder roll, the shoulder pitch and the elbow yaw joints, are controlled by CPGs. The shoulder roll and shoulder pitch joints are controlled by CPG_1 and CPG_2 respectively (Fig. 2), that is, the shoulder pitch joint will be dedicated to the vertical component of motion and its output is the input of the CPG controlling the elbow yaw joint (CPG_3); the shoulder roll joint is responsible for the horizontal part of motion.

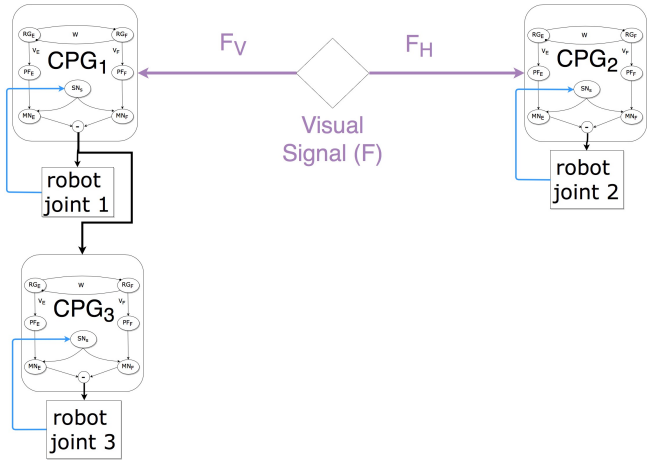

Fig. 2. CPG architecture. The shoulder pitch joint receives the vertical visual signal F_V as an input and its output is the input of the CPG controlling the elbow yaw joint; the shoulder roll joint receives the horizontal visual signal F_H as an input

Moreover, the right CPGs need to be used. For example, while a circular motion requires all joints to be active, the shoulder roll joint or the elbow yaw joint is sufficient for waving. First, the input signal is normalized so that it is always between -1 and 1. The amplitude of the input signal is constantly computed over a moving window of 1 second which allows rapid reconfiguration during the interaction. Then, the output of each CPG is weighted by the movement amplitude in the horizontal or vertical dimension, depending on its specific direction. This scales the movement and "removes" one dimension when the amplitude is too small. The equation of the output thus becomes:

$$\begin{aligned} output_i(t) = &(\max_{t-1 \leq k \leq t} (F_i(k)) - \min_{t-1 \leq k \leq t} (F_i(k))) \\ &\cdot (MN_{i_F} - MN_{i_E}) \end{aligned} \tag{10}$$

IV. Experimental Results

We validate our model with a human - robot interaction for credibility and feasibility's sake. Indeed, human motion has higher variability than theoretical data. And this also illustrates that the CPG is able to compensate the hand detection failings. We demonstrate the CPG capabilities through four different interactions, each highlighting a different aspect: frequency adaptation, movement adaptation, amplitude adaptation, coordinated complex movements.

A. Experimental protocol

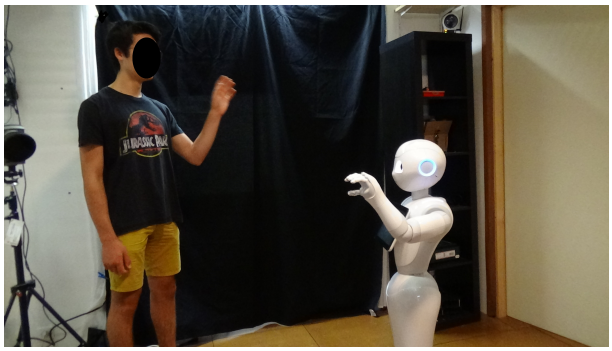

Fig. 3. Experiment setup with the human partner performing rhythmic movements in front of Pepper. Each CPG controls one joint of Pepper to generate rhythmic movements.

Experiments were carried out with the SoftBank Robotics robot Pepper. The code was implemented in Python and run with NaoQi (see Fig. 3). Pepper's front camera provides a visual signal at 10 fps. Using this video stream, the human hand position, obtained with a background subtraction algorithm, is extracted. All image processing steps were performed with OpenCV 3.4. In order to avoid noise (due to lighting) in the detection, Pepper was placed facing a black background. Besides, to ensure a quality signal, some basic image processing steps were additionally performed. First, if needed, the image was enhanced with Contrast Limited Adaptive Histogram Equalization. Then, the hand of Pepper moving in front of the camera could also be wrongly detected as the moving human hand, so an additional thresholding step was added to remove the white parts from the picture, followed by a gaussian blur and morphological opening and closing. Finally, so that the human arm or clothes would not be mistaken for the hand and so that the best possible signal would be obtained, the human partner was also wearing black sleeves (Note that any other color works but the signal

obtained is not as clean). Furthermore, passing the signal through a low-pass filter with 5 Hz cut-off frequency, helps removing detection aberrations.

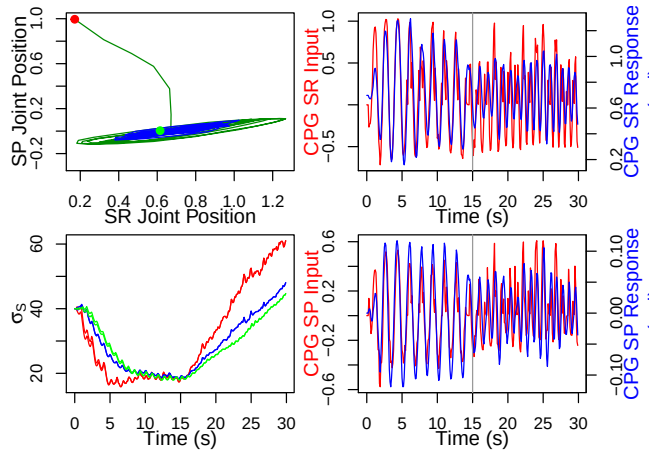

Fig. 4. Top Left: phase portrait of the articular position, in green for the first part (before 15 s) and blue for the second part. Top Right: in red, input of the Shoulder Roll (SR) CPG; in blue, output of the Shoulder Roll (SR) CPG. Bottom Left: σ_S for the Shoulder Roll joint (red), the Shoulder Pitch joint (blue), the Elbow Yaw joint (green). Bottom Right: in red, input of the Shoulder Pitch (SP) CPG; in blue, output of the Shoulder Pitch (SP) CPG

Before the interaction starts, Pepper is at its resting position. If the robot detects a person agitating the arm, it activates the CPGs and responds. Each interaction lasts 30 seconds and human partner was careful to maintain the same movement frequency as much as possible. We designed four interactions to highlight the capacities of the controller (see the associated video [1]).

The parameters used for both experiments are as follows: $\tau_M = 0.35$, $\tau_S = 3.5$, $W = 0.005$, $\sigma_F = 1.0$, $\lambda = 0.02$, $\mu = 5 \cdot 10^{-6}$. They were determined empirically.

B. Frequency Adaptation

The first interaction aims at demonstrating the frequency adaptation abilities of the CPG controller. For that effect, the human will perform one motion slowly for fifteen seconds and then increase the frequency for the remaining time. This can be observed on Figure 4.

The intrinsic frequency of the CPG controller depends on parameter σ_S. On Figure 4, σ_S decreases in the first part of the interaction to adapt to the slow human movement and stabilizes around 10. In the second part of the interaction, it increases to accommodate the fast movement but doesn't stabilize since the human movement is not perfectly homogeneous and the frequency keeps increasing.

C. Amplitude Adaptation

In the second interaction, we will show the amplitude adaptation capacities of the controller. This time, the human will perform a circular gesture and reduce the movement amplitude after fifteen seconds.

[1]The associated video can be found at `https://members.loria.fr/mjouaiti/files/EPIROB19_1.mp4`

The phase portrait of Figure 5 roughly represents the movement performed by the robot. First, the robot is indeed able to achieve a circular motion and two distinct ellipses with different amplitude can be seen. The amplitude adaptation can also be observed in the CPG outputs. The amplitude of the command send to the robot effectively decreases when the human motion amplitude decreases.

Note that the robot is *not* copying the human movement because the amplitude of the robot movement doesn't match the amplitude of the human movement. However as shown previously, if the human reduces the amplitude, the robot will as well.

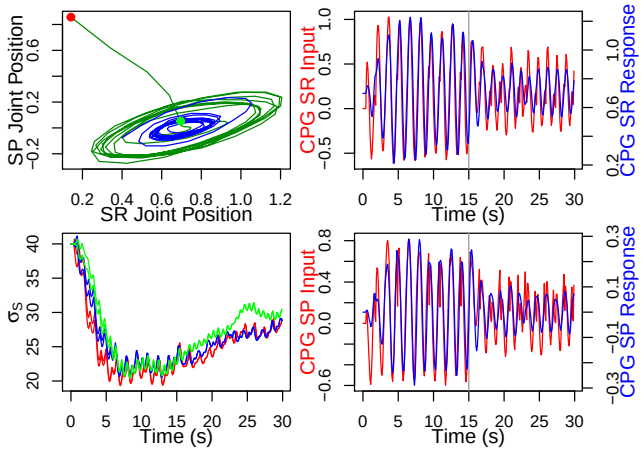

Fig. 5. Top Left: phase portrait of the articular position, in green for the first part (before 15 s) and blue for the second part. Top Right: in red, input of the Shoulder Roll (SR) CPG; in blue, output of the Shoulder Roll (SR) CPG. Bottom Left: σ_S for the Shoulder Roll joint (red), the Shoulder Pitch joint (blue), the Elbow Yaw joint (green). Bottom Right: in red, input of the Shoulder Pitch (SP) CPG; in blue, output of the Shoulder Pitch (SP) CPG

D. Movement Adaptation

We tested the robot on rhythmic motions of three levels of difficulty: easy with waving motion (horizontal/vertical/diagonal), intermediate with a circular motion and difficult with an infinity symbol motion.

In this third interaction, we will highlight the movement adaptation capacities of the controller. This time, the human will switch movement after fifteen seconds. We will not show all the possible movements but we will illustrate the concept.

In the first fifteen seconds, the human performs a horizontal waving gesture and then switches to a circular motion. The two different movements can be observed on the phase portrait of Figure 6. So the controller is able to adapt to different human movements without any reconfiguration of the CPG architecture.

E. Coordinated Complex Movements

In this last part, we show that the controller is able to reproduce complex movements (infinity symbol) and to still achieve coordination. The error measurement metric for coordination between the human and robot movements employed is the Phase Locking Value (PLV) [27]. It ranges

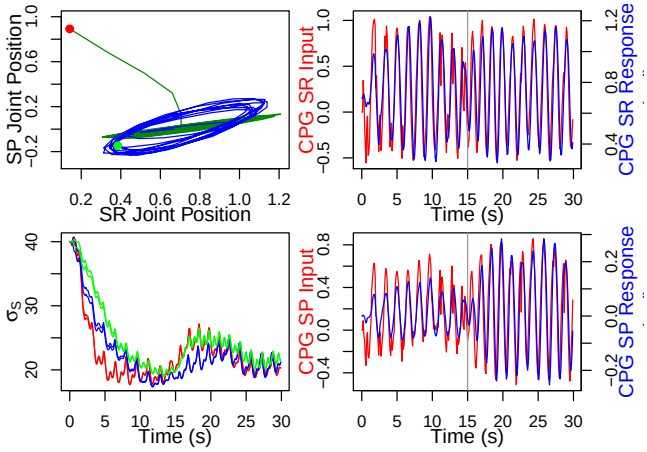

Fig. 6. Top Left: phase portrait of the articular position, in green for the first part (before 15 s) and blue for the second part. Top Right: in red, input of the Shoulder Roll (SR) CPG; in blue, output of the Shoulder Roll (SR) CPG. Bottom Left: σ_S for the Shoulder Roll joint (red), the Shoulder Pitch joint (blue), the Elbow Yaw joint (green). Bottom Right: in red, input of the Shoulder Pitch (SP) CPG; in blue, output of the Shoulder Pitch (SP) CPG

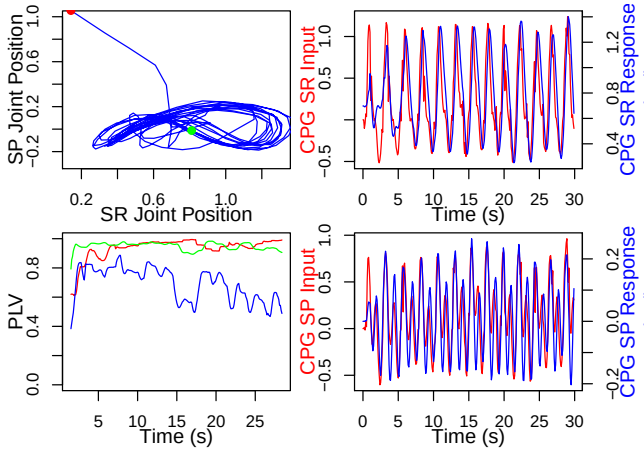

Fig. 7. Top Left: phase portrait of the articular position. Top Right: in red, input of the Shoulder Roll (SR) CPG; in blue, output of the Shoulder Roll (SR) CPG. Bottom Left: PLV for the Shoulder Roll joint (red), the Shoulder Pitch joint (blue), the Elbow Yaw joint (green). Bottom Right: in red, input of the Shoulder Pitch (SP) CPG; in blue, output of the Shoulder Pitch (SP) CPG

from 0 (no coordination) to 1 (perfect coordination). The instantaneous PLV can be defined as:

$$PLV(t) = \frac{1}{N}\left|\sum_{i=0}^{N} e^{j(\phi_1(i)-\phi_2(i))}\right| \tag{11}$$

with N the sliding window size, $j = \sqrt{-1}$, ϕ_k the instantaneous phase of signal k computed with the Hilbert transform.

The PLV for each joint can be observed on Figure 7. Let us remark that the PLV for the Shoulder Pitch joint suggests that the two signals are badly coordinated. However, looking at the curve of the CPG input and output, they appear almost perfectly superimposed. This poor performance can be explained by the fact that the signal is not a perfect sinusoid. Similarly, note also that the PLV sometimes appears crenelated, this is due to the hand position which was sometimes badly detected: these aberrations prevent the human signal from being a perfect sinusoid, which the PLV requires to work optimally.

Moreover, we can observe that the motion performed by the robot is not perfectly symmetrical. This is due to the human motion not being symmetrical either. The CPG maintains human characteristics.

V. Discussion and Conclusion

This paper demonstrated the versatility of our model of plastic CPG for motor coordination learning between a robot and a human partner over a wide range of movements.

Results show that the robot achieves motor coordination with the human partner through a visual signal of a hand performing rhythmic movements. The robot is able to adapt its frequency, amplitude and motion generation according to the human motion. However, we do not achieve copying of the motion but rather, the robot adapts to the frequency and movement while retaining its own identity. This is similar to what we observed in on-going research of human interactions where individuals perform the same movement at the same frequency but each maintaining their own characteristics.

Moreover, in our previous case study of handshaking [24], the CPG was entrained due to the physical locking. In this case, there is no physical contact so plasticity mechanisms truly are responsible for the motor coordination and adaptation. Were σ_s not learned, the robot would just move at its own intrinsic frequency and there would be no coordination whatsoever with the human partner.

Note also that in [24], we used force feedback and the CPG output as a velocity command. Here, as there is no physical interaction and the Pepper robot has neither velocity control nor torque sensors, a similar setup could not possibly be done. However, we still employ the same CPG successfully, thus demonstrating its versatility and the wide range of possibilities. Moreover, in on-going research, we are also able to use the CPG output as a torque command.

Our system allows us to control the robot in real time since our calculations are very fast: the CPG calculations last under 5 ms and the image processing around 20 ms.

The scope of this work needn't restrain itself to mere arm motion. Pepper is a social robot and is more and more used as such. Nowadays, it can be found in train stations, shopping centers, hospitals, schools... This work could easily be generalized to another set of joints or another robot to realize any synchronized rhythmic actions. This could be taken much further with whole-body coordination using music or while "walking". People already tend to interact with Pepper easily because of its appealing appearance; a coordinated, more "human-like", dare we say, interaction might still enhance the quality of the experience.

In future works, we plan to reproduce discrete movements as well as rhythmic movements and be able to switch seamlessly between both. We will also improve the detection quality and robustness and generalize it to expand this work to whole upper-body control.

REFERENCES

[1] E. Delaherche, M. Chetouani, A. Mahdhaoui, C. Saint-Georges, S. Viaux, and D. Cohen, "Interpersonal synchrony: A survey of evaluation methods across disciplines," *IEEE Transactions on Affective Computing*, vol. 3, no. 3, pp. 349–365, 2012.

[2] A. Z. Zivotofsky and J. M. Hausdorff, "The sensory feedback mechanisms enabling couples to walk synchronously: An initial investigation," *Journal of neuroengineering and rehabilitation*, vol. 4, no. 1, p. 28, 2007.

[3] A. P. Demos, R. Chaffin, K. T. Begosh, J. R. Daniels, and K. L. Marsh, "Rocking to the beat: Effects of music and partner's movements on spontaneous interpersonal coordination.," *Journal of Experimental Psychology: General*, vol. 141, no. 1, p. 49, 2012.

[4] G. Tagne, P. Hénaff, and N. Gregori, "Measurement and analysis of physical parameters of the handshake between two persons according to simple social contexts," in *Intelligent Robots and Systems (IROS), 2016 IEEE/RSJ International Conference on*, pp. 674–679, 2016.

[5] K. Yonekura, C. H. Kim, K. Nakadai, H. Tsujino, and S. Sugano, "A role of multi-modal rhythms in physical interaction and cooperation," *EURASIP Journal on Audio, Speech, and Music Processing*, vol. 2012, no. 1, p. 12, 2012.

[6] N. F. Troje, J. Sadr, H. Geyer, and K. Nakayama, "Adaptation aftereffects in the perception of gender from biological motion," *Journal of vision*, vol. 6, no. 8, pp. 7–7, 2006.

[7] C. N. Macrae, O. K. Duffy, L. K. Miles, and J. Lawrence, "A case of hand waving: Action synchrony and person perception," *Cognition*, vol. 109, no. 1, pp. 152–156, 2008.

[8] D. Pongas, A. Billard, and S. Schaal, "Rapid synchronization and accurate phase-locking of rhythmic motor primitives," in *Intelligent Robots and Systems, 2005.(IROS 2005). 2005 IEEE/RSJ International Conference on*, pp. 2911–2916, IEEE, 2005.

[9] A. J. Ijspeert, J. Nakanishi, and S. Schaal, "Learning rhythmic movements by demonstration using nonlinear oscillators," in *Proceedings of the ieee/rsj int. conference on intelligent robots and systems (iros2002)*, no. BIOROB-CONF-2002-003, pp. 958–963, 2002.

[10] E. Ansermin, G. Mostafaoui, N. Beaussé, and P. Gaussier, "Learning to synchronously imitate gestures using entrainment effect," in *International conference on simulation of adaptive behavior*, pp. 219–231, Springer, 2016.

[11] S. Schaal, "Dynamic movement primitives-a framework for motor control in humans and humanoid robotics," in *Adaptive motion of animals and machines*, pp. 261–280, Springer, 2006.

[12] E. P. Zehr, T. J. Carroll, R. Chua, D. F. Collins, A. Frigon, C. Haridas, S. R. Hundza, and A. K. Thompson, "Possible contributions of cpg activity to the control of rhythmic human arm movement," *Canadian journal of physiology and pharmacology*, vol. 82, no. 8-9, pp. 556–568, 2004.

[13] S. Grillner and P. Wallen, "Central pattern generators for locomotion, with special reference to vertebrates," *Annual review of neuroscience*, vol. 8, no. 1, pp. 233–261, 1985.

[14] K. Matsuoka, "Mechanisms of frequency and pattern control in the neural rhythm generators," *Biological cybernetics*, vol. 56, no. 5-6, pp. 345–353, 1987.

[15] E. Hopf, "Abzweigung einer periodischen lösung von einer stationären lösung eines differentialsystems," *Ber. Math.-Phys. Kl Sächs. Akad. Wiss. Leipzig*, vol. 94, pp. 1–22, 1942.

[16] P. F. Rowat and A. I. Selverston, "Modeling the gastric mill central pattern generator of the lobster with a relaxation-oscillator network," *Journal of neurophysiology*, vol. 70, no. 3, pp. 1030–1053, 1993.

[17] J. Nassour, T. D. Hoa, P. Atoofi, and F. Hamker, "Concrete action representation model: from neuroscience to robotics," *IEEE Transactions on Cognitive and Developmental Systems*, 2019.

[18] E. Marder and D. Bucher, "Central pattern generators and the control of rhythmic movements," *Current biology*, vol. 11, no. 23, pp. R986–R996, 2001.

[19] I. A. Rybak, K. J. Dougherty, and N. A. Shevtsova, "Organization of the mammalian locomotor cpg: Review of computational model and circuit architectures based on genetically identified spinal interneurons(1,2,3)," *eNeuro*, vol. 2, Sep. 2015.

[20] J. Nassour, P. Hénaff, F. Benouezdou, and G. Cheng, "Multi-layered multi-pattern cpg for adaptive locomotion of humanoid robots, biological cybernetics," *Biological cybernetics*, vol. 108, no. 3, pp. 291–303, 2014.

[21] S. Debnath, J. Nassour, and G. Cheng, "Learning diverse motor patterns with a single multi-layered multi-pattern cpg for a humanoid robot," in *Humanoid Robots (Humanoids), 2014 14th IEEE-RAS International Conference on*, pp. 1016–1021, IEEE, 2014.

[22] S. M. Danner, S. D. Wilshin, N. A. Shevtsova, and I. A. Rybak, "Central control of interlimb coordination and speed-dependent gait expression in quadrupeds," *The Journal of physiology*, vol. 594, no. 23, pp. 6947–6967, 2016.

[23] W. W. Teka, K. C. Hamade, W. H. Barnett, T. Kim, S. N. Markin, I. A. Rybak, and Y. I. Molkov, "From the motor cortex to the movement and back again," *PloS one*, vol. 12, no. 6, p. e0179288, 2017.

[24] M. Jouaiti, L. Caron, and P. Hénaff, "Hebbian plasticity in cpg controllers facilitates self-synchronization for human-robot handshaking," *Frontiers in Neurorobotics*, vol. 12, p. 29, 2018.

[25] L. Righetti, J. Buchli, and A. J. Ijspeert, "Dynamic hebbian learning in adaptive frequency oscillators," *Physica D: Nonlinear Phenomena*, vol. 216, no. 2, pp. 269–281, 2006.

[26] S. I. Fried and R. H. Masland, "Image processing: how the retina detects the direction of image motion," *Current Biology*, vol. 17, no. 2, pp. R63–R66, 2007.

[27] J.-P. Lachaux, E. Rodriguez, J. Martinerie, F. J. Varela, *et al.*, "Measuring phase synchrony in brain signals," *Human brain mapping*, vol. 8, no. 4, pp. 194–208, 1999.